JOURNAL OF MATERIALS SCIENCE **39** (2004) 3739– 3744

Preparation of nanocrystalline $SrBi_2Ta_2O_9$ powders using sucrose-PVA as the polymeric matrix

A. B. PANDA, A. TARAFDAR, S. SEN, A. PATHAK, P. PRAMANIK*
Department of Chemistry, Indian Institute of Technology, Kharagpur-721302, West Bengal, India
E-mail: ami@chem.iitkgp.ernet.in

Nanocrystalline powders of $SrBi_2Ta_2O_9$ (Strontium Bismuth Tantalate) have been prepared through evaporation of a polymer-based aqueous precursor solution. The precursor solution was obtained by homogeneous dispersion of the water-soluble metal salts (i.e., strontium nitrate, bismuth nitrate and tartarate complex of tantalum) in a polymeric matrix created by an aqueous solution mixture of sucrose and polyvinyl alcohol. Complete evaporation of the precursor solution (at ~200°C) resulted in a fluffy, porous, carbonaceous mass, which on calcination at 750°C/2 h yield the single-phase $SrBi_2Ta_2O_9$ powders with average particle size ~35 nm. The compacted powders, after sintering at 1000°C/4 h, show density of 96.8% of its theoretical value and dielectric constant value of 862 with Curie temperature (T_c) at 287°C, when measured at 100 KHz.

1. Introduction

Ferroelectrics, which can retain their polarization state after the removal of applied field, have been intensively investigated for application in nonvolatile ferroelectric random access memory (NVFRAM) device fabrications [1]. Lead zirconate titanates [i.e., PZT(s)] are the most widely used ferroelectric materials for this purpose, but their application in such devices are impeded by their serious degradation switching i.e., fatigue [2]. The ferroelectrics, 'Strontium Bismuth Tantalate' (i.e., SBT), discovered by Aurivillius in 1949 and their ferroelectric properties and basic structure studied by Subbarao and Smolenskii in early 60's, have in contrast been reported to exhibit fatigue endurance even after 10^{12} cycles of operation with excellent retention characteristics [3, 4]. With this discovery, a class of promising ferroelectrics for NVFRAM applications has been recognized that has minimal polarization fatigue and can use low polarization switching voltages. SBT is a layered perovskite type ferroelectric material [5] where two pseudo-perovskite type TaO_6 octahedrons are stacked between alternating layers of $(Bi_2O_2)^{2+}$, along the c-axis, while the strontium ions lie in the space between the TaO_6 octahedrons [6]. The crystal structure has orthorhombic symmetry with $a = 0.5306$ nm, $b = 0.55344$ nm, and $c = 2.49839$ nm; and the theoretical density is 8.785 g cm^{-3}. The spontaneous polarization in SBT, arising from the $(SrTaO_3)^{1+}$ group, lies parallel to the $(Bi_2O_2)^{2+}$ layer (in the a- and b-axis direction). The $(Bi_2O_2)^{2+}$ layers are thought to serve as shock absorbers for enduring the polarization fatigue by weakening the dipole interactions between the perovskite building blocks [7].

Extensive studies have been reported on the various techniques of preparation of SBT thin films for the FeRAM application [8–12] but there is limited literature available on the preparation and characterization of SBT powders [13–18].

Similar to any other ceramic composition, the properties of STB(s) are greatly influenced by their powder characteristics. Thus, wet chemical processes that ensures chemical homogeneity and stoichiometric control in the final compositions through molecular level mixing of the starting materials in the solution [19, 20] are regarded to be the most suitable methods for their preparation. Sol-gel [17, 18] and the colloid emulsion [15] methods are considered to be the most competent chemical processes for the preparation of SBT powders. However, these non-aqueous based solution methods are constrained by the high cost, moisture sensitivity, and scarcity of the starting materials (e.g., the alkoxides). Again, the alternative aqueous based chemical processes get complicated due to non-availability of stable, water-soluble salts of the V(b) group metals [i.e., Ta^{+5}]. According to recent literature reports on the preparation of SBT type ceramic compositions, the problems associated with the starting materials for V(b) group metal ions can be overcome by using their coordinating complexes [21, 22] that are stable in aqueous medium and can be prepared using commonly available laboratory reagents.

*Author to whom all correspondence should be addressed.

In this present paper, we report the synthesis of nanocrystalline SBT powders through thermolysis of a polymer-based aqueous precursor solution process, where water-soluble coordinating tantalum-tartarate complex has been used as the source of tantalum. The aqueous precursor solution is composed of stoichiometric amounts of tantalum-tartarate complex, bismuth nitrate, and strontium nitrate, dispersed in the polymeric matrix provided by an aqueous solution mixture of 10%(w/v) polyvinyl alcohol (PVA) and sucrose. Thermolysis of the precursor solution results in voluminous, fluffy carbonaceous precursors and their calcination at 750°C/2 h yield the desired SBT phase. The precursor and calcined powders have been characterized by thermal analysis (TG and DTG), X-ray diffraction (XRD), and transmission electron microscopy (TEM). Dielectric properties of the sintered pellets of the calcined powders have been measured and the chemical analysis of the pellets has been carried out by energy dispersive X-ray analysis (EDAX).

2. Experimental procedure

The raw materials that were used for the preparation of the ceramic SBT were $Sr(NO_3)_2$ (MERCK, India), $Bi(NO_3)_3$ (BDH, India), polyvinyl alcohol (average molecular weight 1,25,000 Daltons; MERCK, India), sucrose, and tantalum-tartarate complex. The solution of the tantalum-tartarate complex was prepared in the laboratory from tantalum pentoxide (Ta_2O_5, Aldrich) and the details of the preparation process are discussed elsewhere [23].

In the preparation of $SrBi_2Ta_2O_9$ (SBT), appropriate volumes of aqueous solutions of $Sr(NO_3)_2$, and $Bi(NO_3)_3$ were taken from their freshly prepared stocks and mixed together. A stoichiometric amount of the prepared tantalum-tartarate complex solution was then introduced into the solution mixture, followed by the addition of aqueous solutions of 10% (w/v) PVA (∼3 moles of monomer units, with respect to the total moles of the metal ions), and sucrose (∼4 moles with respect to the total moles of the metal ions). Finally, a clear, homogeneous precursor solution was obtained through continuous stirring of the solution mixture while maintaining the pH ≈ 5 by adding dilute HNO_3. Complete evaporation of the precursor solution generated a mass with a characteristic black color. Thermolysis of this mass on a hot plate (at 200°C) resulted in crushable, fluffy, carbonaceous precursors. Calcination of the carbonaceous precursors at selected temperatures (ranging between 500–900°C) resulted in the nanocrystalline SBT powders. The entire preparative process has been illustrated in Fig. 1. Thermal studies of 6.5 mg of the virgin carbonaceous precursors were carried out at a heating rate of 5°C/min, using a simultaneously recording thermo-gravimetric and differential thermal analysis (i.e., TG and DTA) (model DT-40, Shimadzu, Kyoto, Japan). Phase analysis of the samples (after calcination at various temperatures) was carried out using a X-ray powder diffractometer (XRD) (Phillips PW-1804, Netherlands). Powder morphology was examined by transmission electron microscopy (TEM) using model TM 300, Phillips, and the dielectric properties of the sintered pellets were measured using a capacitance-measuring assembly (model AP-1620, GRC).

3. Results and discussion

3.1. Thermal analysis

Thermal analysis of the virgin carbonaceous precursors is shown in Fig. 2. DTA curve initially showed a small endothermic effect (between A–B) probably due to desorption of water. Thereafter, the DTA curve showed a monotonic increase in the heat output (between

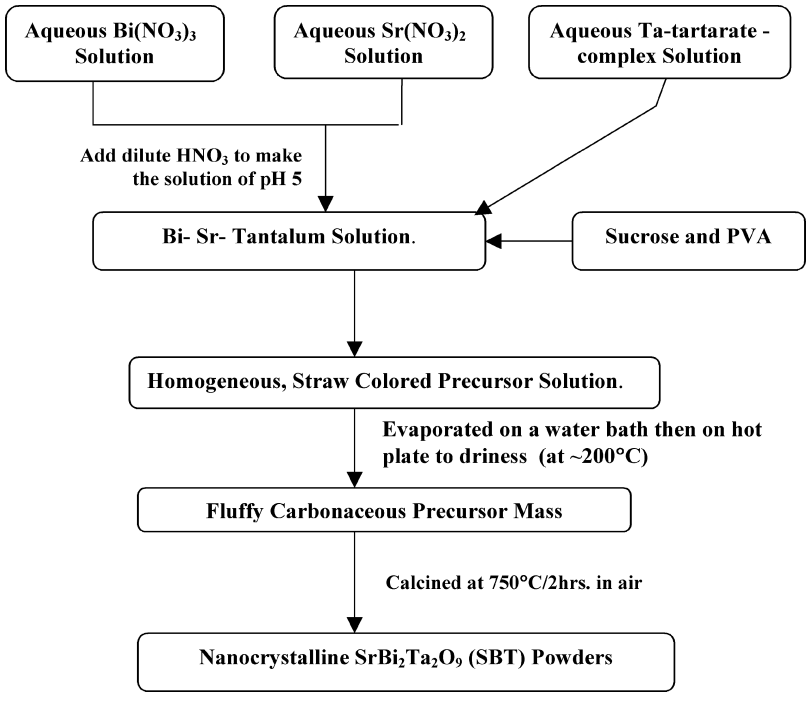

Figure 1 Schematic representation of the preparation of $SrBi_2Ta_2O_9$ nanocrystalline powders through the sucrose-PVA polymer matrix precursor solution method.

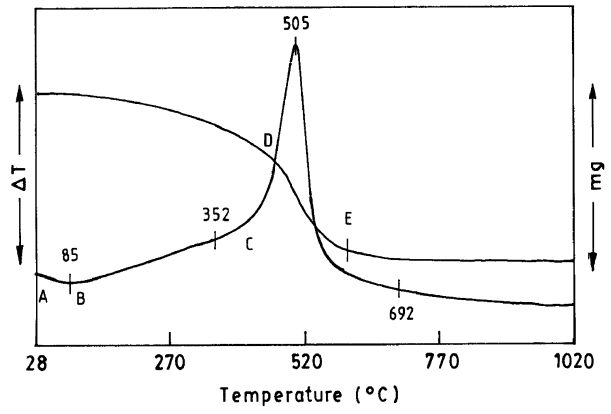

Figure 2 Thermal studies of the $SrBi_2Ta_2O_9$ precursors powders.

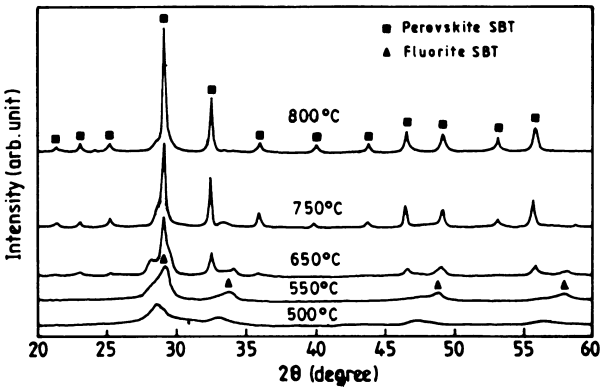

Figure 3 X-ray diffractograms (using $Cu\,K_\alpha$ radiation) of the $SrBi_2Ta_2O_9$ precursors on heat-treatment for two hours at: 500°C, 550°C, 650°C, 750°C, and 850°C.

B–C) with an exothermic peak at 505°C, possibly due to combustion of the residual carbon in the precursor powders along with crystallization of the SBT phase. The concurrence of the two processes implied that the heat generated from the combustion of residual carbon facilitated the formation of the nanocrystals of the oxide phase. The TG curve showed that the entire thermal effect was manifested by a single step weight loss of ∼35% up to ∼600°C. Beyond 600°C the TG curve remained constant inferring the samples to be carbon free.

3.2. XRD analysis

XRD analysis of the precursor and their respective calcined powders (calcined at different temperatures ranging from 500–900°C/2 h) were performed to study the effect of heat-treatment temperatures on the formation of the layered perovskite-SBT phase (see Fig. 3). The virgin SBT precursors were observed to be amorphous to X-ray whereas calcination of these precursors between 500 and 650°C, revealed the formation of the Fluorite-SBT phase [21]. Calcination of the precursors above 650°C was marked by diminishing intensity of the diffraction lines corresponding to the fluorite phase and appearance of characteristic diffraction lines of the perovskite-SBT phase. At 750°C the fluorite phase was completely transformed into the pure perovskite SBT phase. Thus, the Fluorite-SBT phase appeared to be the nucleating phase for the crystallization of the pure perovskite-SBT phase.

The crystallite size of the calcined powders, calculated from X-ray line broadening studies using the Scherrer's equation [24], was found to be ∼17 nm. The crystallite sizes of the SBT powders were observed to increase with the rise in the calcination temperatures.

The minimum temperature required for the formation of the pure SBT phase through calcination of the respective virgin precursors was found to be 750°C, which is lower than those reported through the solid-state method though almost comparable to those reported through other aqueous based solution methods. Table I presents a comparative study of the perovskite phase formation temperatures in $SrBi_2Ta_2O_9$ composition when synthesized through various processes. The low external heat-treatment temperatures, required for the realization of the perovskite-SBT phase through the present method, may possibly be due to the presence of small atomic clusters of appropriate chemical homogeneity in the amorphous precursors that facilitate the crystallization process.

3.3. TEM analysis

The bright field transmission electron micrographs of the SBT powders, after heat-treatment of the precursor powders at its phase formation temperatures (i.e., at 750°C/2 h), are illustrated in Fig. 4a. The bright field TEM micrographs represent the basic powder morphology of the sample, where the smallest visible isolated spot can be identified as particle/crystallite agglomerates. From the TEM study of the SBT powders, it was

TABLE I Comparison of the SBT phase formation temperatures and the average particle sizes for the $SrBi_2Ta_2O_9$ composition as reported in the other synthesis processes

Method of preparation	[a]Formation temp. (°C)	[b]Average particle size	Sintering temp. (°C)	T_C (°C)	Dielectric constant at T_C
1. Present method	750/2 h	∼35 nm	1000	287	862
2. Colloidal emulsion method [15]	750/2 h	∼60 nm	–	–	–
3. Sol-gel method [17]	650/2 h	∼70 nm	–	–	–
4. Solid state double calcination method [14]	800/2 h	0.50–0.15 μm	–	–	
5. Solid state method [16]	900/5 h	1–4 μm	1150	290	475

[a]Calcination temperature required for the formation of the perovskite SBT phase for the $SrBi_2Ta_2O_9$ composition.
[b]Average particle size reported at the respective perovskite SBT phase formation temperatures.

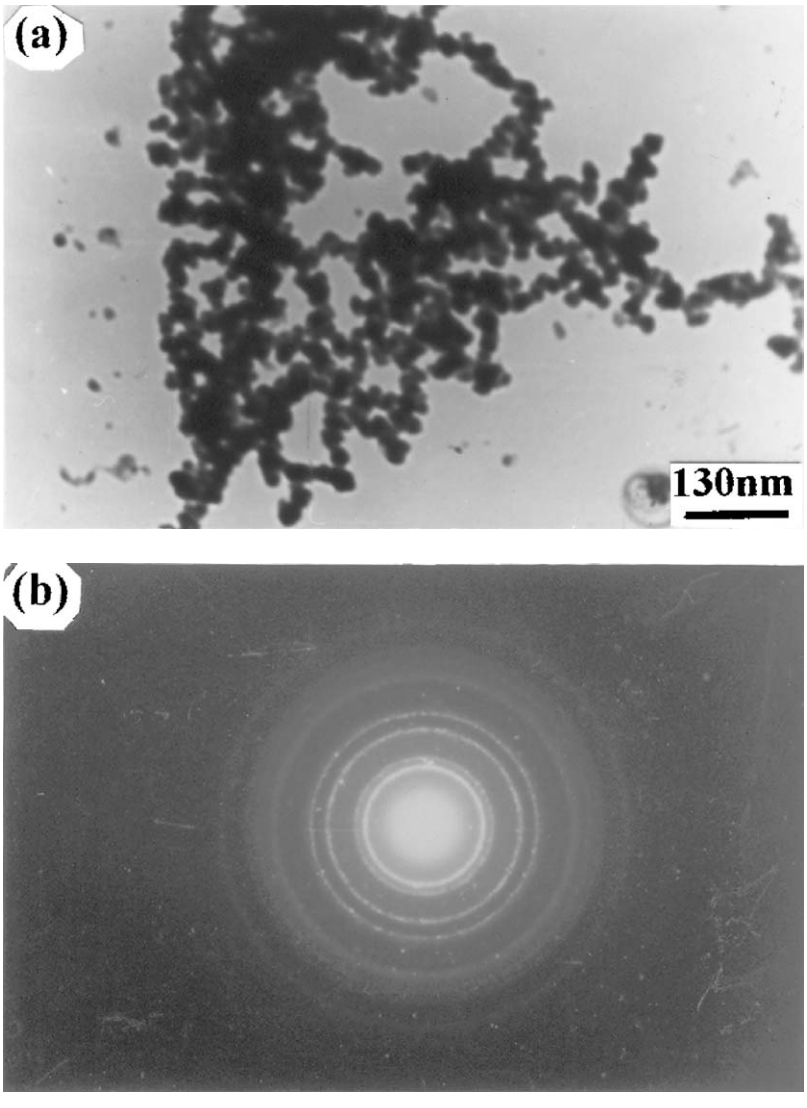

Figure 4 (a) Bright field transmission electron micrograph of the $SrBi_2Ta_2O_9$ samples after calcination of the precursor powders at 750°C/2 h. (b) The corresponding selected area electron diffraction (SAED) pattern of the $SrBi_2Ta_2O_9$ powders after calcination of the precursor powders at 750°C/2 h.

observed that the particles are almost spherical with average particle diameter ~35 nm. The corresponding selected area electron diffraction pattern of the same sample showed distinct rings, which is characteristic of an assembly of nano-crystallites (Fig. 4b).

3.4. Sintering studies

The SBT nanocrystalline powders (calcined at 750°C/2 h) were compacted into pellets by applying a uni-axial pressure of 3.2×10^7 Pa and then sintered at temperatures 900–1100°C/4 h. Density measurements for the sintered SBT pellets were carried out through Archimedes' method. The change in density of the SBT pellets with sintering temperature is illustrated in Fig. 5. From the graph it is evident that the density of the pellet was 96.8% of its theoretical value at the sintering temperature of 1000°C. Sintering of the pellets at or above 1050°C increased the density to the maximum value of 97.4% but it also promoted the evaporation of Bi_2O_3 from the system, which led to non-stoichiometries in the SBT composition. The loss of bismuth from the system was inferred by the appearance of bismuth deficit phase in the X-ray diffractograms of the corresponding sintered pellet (Fig. 6).

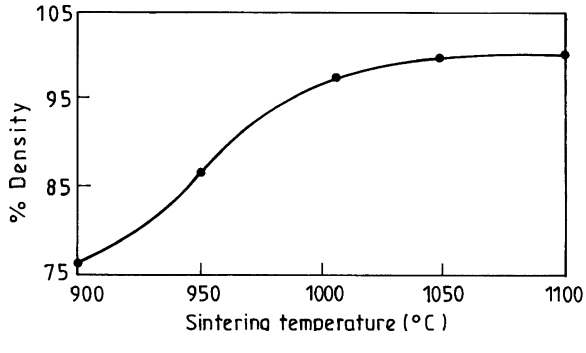

Figure 5 Variation in sintered density of the pressed pellet (using powders calcined at 750°C/2 h) with sintering temperature.

3.5. Dielectric studies

Dielectric constant measurements were performed on the pellets that were sintered at 1000°C and had a relative density of 96.8%. Both sides (i.e., the flat surface) of the sintered pellet were polished and then electroded by applying a silver paste. Variation of dielectric constant (ε) and dielectric loss with temperature, at a frequency of 100 kHz, was studied for the pellet and their results are depicted in Fig. 7. The study revealed that the dielectric constant increased gradually with temperature

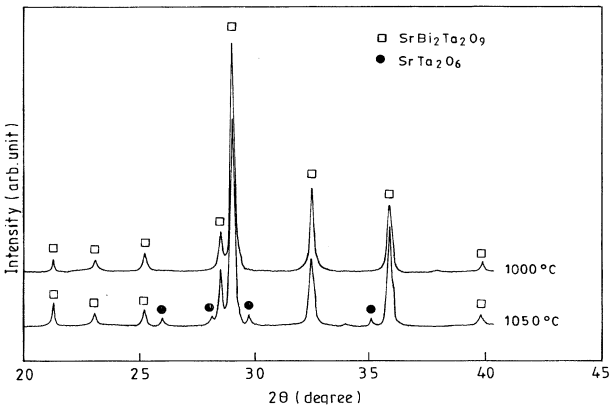

Figure 6 X-ray diffractograms (using Cu K_α radiation) of the SBT pellets sintered at (a) 1000°C and (b) 1050°C.

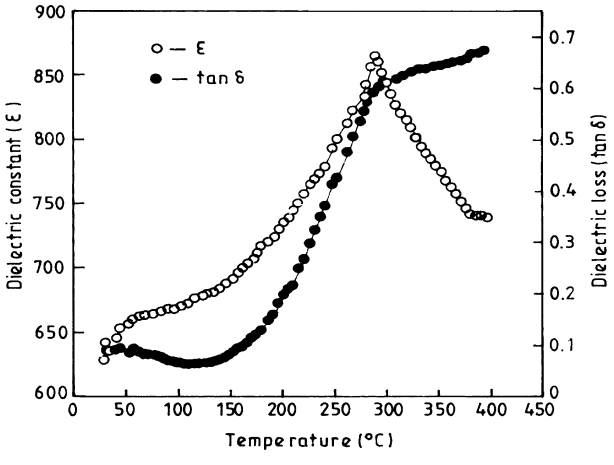

Figure 7 Variation of dielectric constant (ε) and dielectric loss (tan δ) with temperature for the SBT pellets, sintered at 1000°C.

and reached a maximum (ε_{max}) at the Curie temperature (T_c), typical of any normal ferroelectric material. The ε_{max} value, measured at 100 kHz, was found to be 862 at the Curie temperature (T_c) of 287°C, which is higher than those reported through the solid-state method [16]. Again, as expected for normal ferroelectrics, the temperature at which the dielectric constant peaks (at a frequency of 100 kHz) was found to almost coincide with the point of inflection observed in the dielectric loss versus temperature plot.

Variation of dielectric constant and dielectric loss as a function of frequency, for the sintered (at 1000°C for 2 h) SBT pellet, has been shown in Fig. 8. It shows that both, the dielectric constant and the dielectric loss decrease drastically with increase in frequency, as in normal ferroelectrics.

3.6. Discussion on the developed method of preparation

In the developed process, the aqueous solution mixture of sucrose and PVA in the precursor solution provides a polymeric matrix with molecular scale dispersion of metal ions. Sucrose plays a multifarious role in this process. It coordinates through its hydroxyl groups to form complexes with the metal ions that remain in solution through formation of small micelle-type moieties. These micelle-type structures circumvent selective precipitation of the cations during the evaporation process by keeping them trapped inside such moieties. Moreover, sucrose being in excess to the cations behaves as a strong chelating agent and ensures atomic level distribution of the cations through the polymeric network. During the evaporation of the precursor solution, sucrose possibly gets hydrolyzed to fructose and glucose in the presence of nitric acid, which ultimately gets oxidized to gluconic acid and then to polybasic acids, which forms a branched polymer with PVA [25].

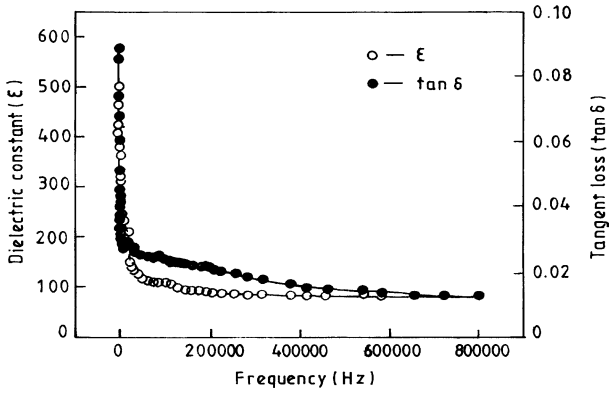

Figure 8 Room temperature studies on the variation of dielectric constant (ε) and dielectric loss (tan δ) with frequency for the SBT pellets, sintered at 1000°C.

$$C_{12}H_{22}O_{11}(\text{Sucrose}) + H_2O \xrightarrow[\Delta]{H^+} C_6H_{12}O_6(\text{glucose}) + C_6H_{12}O_6\ (\text{fructose})$$

$$\downarrow$$

$$\text{Branched polymer} \leftarrow \text{PVA} + C_6H_{12}O_7\ (\text{gluconic acid})$$

Complete evaporation of this polymeric material results in a highly porous, fluffy carbonaceous precursor material, and the metal oxides remain embedded in the matrix of the mesoporous carbon. Calcination of the precursors at relatively low external temperatures results in the formation of SBT nanocrystals with controlled crystallite size. The decomposition of carbonaceous material produced gasses (such as: CO, CO_2, NH_3, NO_2, and water vapor), which not only helped to disintegrate the agglomerated particles but also helped to inhibit sintering of the nanosized particles.

4. Conclusions

A simple aqueous-based chemical route involving a polymeric matrix of sucrose and polyvinyl alcohol is explored for synthesizing nanocrystals of $SrBi_2Ta_2O_9$, using cost-effective, easily available and water-soluble starting materials. Stable, water-soluble coordinated tartarate complex of tantalum has been used as the source of tantalum. The polymeric matrix used in this method serves as a solid dispersoid for the metal ions in an acidic precursor solution as well as a solid fuel during the calcination of the precursor. Decomposition of the polymeric matrix initiated during the evaporation process and resulted in fluffy, carbonaceous precursors that had the metal oxides embedded in its porous template. The carbonaceous residue from the polymeric

reagent acted as an efficient internal fuel during the calcination process and the heat generated during such as a exothermic oxidative process resulted in the formation of pure $SrBi_2Ta_2O_9$ layered perovskite, via the intermediate fluorite phase, at external temperatures as low as 750°C with particle size ~35 nm.

The developed low-temperature process yields the smallest particle sizes of $SrBi_2Ta_2O_9$ compared to those reported through all the other routes while their dielectric properties showed a reasonable increment in comparison to those report through the solid-state process.

This process should be applicable to the preparation of nanosized powders of any tantalum based ferroelectric compositions.

Acknowledgment

The authors are grateful for the financial assistance for this study from the Council of Scientific and Industrial Research (CSIR), Government of India.

References

1. J. F. SCOTT and C. A. ARAUJO, *Science* **246** (1989) 1400.
2. G. A. C. M. SPIERINGS, M. J. E. ULENAERS, G. L. M. KAMPSCHO'ER, H. A. M. VAN HAL and P. K. LARSEN, *J. Appl. Phys.* **70** (1991) 2290.
3. C. A. DE ARAUJO PAZ, J. D. CUCHIARO, M. C. SCOTT and L. D. MCMILLAN, *International Patent* **WO93** (1993) 12542.
4. J. F. SCOTT, F. M. ROSS, C. A. DE ARAUJO PAZ, M. C. SCOTT and M. HOFFMAN, *M. R. S. Bull.* **21** (1996) 33.
5. B. AURIVILLIUS, *Arkiv Für Kem* **54** (1949) 483.
6. E. C. SUBBARAO, *J. Phys. Chem. Solids* **23** (1962) 665.
7. K. KATO, C. ZHENG, J. M. FINDER, S. K. DEY and K. TORII, *J. Amer. Ceram. Soc.* **81**(7) (1998) 1869.
8. M. L. CALZADA, A. GONZALEZ, R. JIMENEZ, C. ALEMANY and J. MENDIOLA, *J. Eu. Ceram. Soc.* **21** (2001) 1517.
9. A. GRUVERMAN, A. PIGNOLET, K. M. SATYALAKSHMI, M. ALEXE, N. D. ZAKHAROV and D. HESSE, *Appl. Phys. Lett.* **76**(1) (2000) 106.
10. S. B. DESU, D. P. VIJAY, X. ZANG and B. P. HE, *ibid.* **69**(12) (1996) 1719.
11. K. KATO, C. ZHENG, J. M. FINDER, S. K. DEY and K. TORII, *J. Amer. Ceram. Soc.* **81**(7) (1998) 1869.
12. P. Y. CHU, R. E. JONES JR, P. ZURCHER, D. J. TAYLOR, B. JIANG, S. L. GILLESPIE and Y. T. LII, *J. Mater. Res.* **11**(5) (1996) 1065.
13. Y. SHIMAKAWA, Y. KUBO, Y. NAKAGAWA, S. GOTO, T. KAMIYAMA, H. ASANO and F. IZUMI, *Phys. Rev.* B **61**(10) (2000) 6559.
14. C. H. LU and J. T. LEE, *Ceram. Inter.* **24** (1998) 285.
15. C. H. LU and S. K. SAHA, *J. Amer. Ceram. Soc.* **83**(5) (2000) 1320.
16. J. S. KIM, C. CHEON, H. S. SHIM and C. H. LEE, *J. Eu. Ceram. Soc.* **21** (2001) 1295.
17. Q. F. ZHOU, H. L. W. CHAN and C. L. CHOY, *J. Non-Cryst. Solids* **254** (1999) 106.
18. D. RAVICHANDRAN, K. YAMAKAWA, A. S. BHALLA and R. ROY, *J. Sol-Gel Sci. Techn.* **9**(1) (1997) 95.
19. R. N. DAS, A. PATHAK and P. PRAMANIK, *J. Amer. Ceram. Soc.* **81**(12) (1998) 3357.
20. J. C. ROY, R. K. PATI and P. PRAMANIK, *J. Eu. Ceram. Soc.* **20** (2000) 1289.
21. D. NELIS, K. V. WERDE, D. MONDELAERS, G. VANHOLAND, M. K. V. BAEL, J. MULLENS and L. C. V. POUCKE, *ibid.* **21** (2001) 2047.
22. R. N. DAS and P. PRAMANIK, *NanoStruct. Mater.* **11**(3) (1999) 325.
23. A. B. PANDA, A. PATHAK, M. L. NANDAGOSWAMI and P. PRAMANIK, *Mater. Sci. Eng.* B **B97** (2003) 275.
24. M. P. KLUG and L. E. ALEXANDER, "X-ray Diffraction Procedure for Polycrystalline and Amorphous Material" (Wiley, New York, 1974) p. 634.
25. P. PRAMANIK, *Bull. Mater. Sci.* **18** (1995) 819.

Received 22 October 2002
and accepted 5 March 2004